

Studies of all order correlation effects in the isotope shifts and fine structure variation constants: Applications to Na and Mg⁺

B. K. Sahoo *

Theoretical Physics Divison, Physical Research Laboratory, Ahmedabad-380009, India

(Dated: February 20, 2018)

We study the electron correlation effects in the calculations of isotope shifts in Na and Mg⁺ using the relativistic coupled-cluster method. The trends of the correlation effects are explicitly discussed and comparison of the present results with the previously reported results are given. We also present the fine structure constant variation coefficients for many states in the above systems. From these results, it is possible to find out suitable transition lines those can be used as anchor and probe lines in finding possible variation in the fine structure constant.

PACS numbers:

Keywords:

I. INTRODUCTION

Study of isotope shifts (ISs) in atomic systems has been a long time immense interest to the physicists [1–4]. It is a challenging problem to find out the role of the correlation effects in the IS calculations using an *ab initio* approach for a system involving more than three electrons. The most difficult part in IS determination lies in calculating the specific mass shift (SMS) which involves two-body interactions between the electron momenta [1, 2] and treating correlation effects to all orders in this property is as difficult as considering the Coulomb interaction between the electrons. Often semi-empirical methods [3, 5] have been used to calculate these properties without describing the electron correlation behaviors. There have been a number of works carried out using the non-relativistic theories to include the correlation effects that consider particular type of correlation effects to all orders and some of the correlation effects are taken only up to finite order [6–10].

Studies of ISs are important in a number of applications ranging from nuclear physics to astrophysics [3, 5, 11–15]. Accurate determination of these quantities in combinations with the corresponding measurements can be used to extract the relative root mean square (rms) nuclear charge radii of different isotopes that cannot be measured directly [3, 5]. They are also used to test various nuclear models [11, 12]. Since the rms radii variation in the considered systems can be determined precisely using the nuclear models due to small sizes of their nuclei, we will not focus our studies in that direction here. Again, some of the ISs are also used to probe the isotopic abundances of different elements in the astronomical objects [14, 15].

In another context, it is believed that there is possibility of space-time variation of the fine-structure constant $\alpha = e^2/hc$ at the cosmological scale [16–18]. This can be verified by analyzing the quasar absorption spectra

[19–22]. It is also possible to find out any variation of α by comparing the measurements of the ratios of the fine structure intervals to the optical transition frequencies in the laboratory experiments and that from some distant astrophysical objects [23–25]. Any difference in these results can be related to the space-time variation of α . However, the frequency shifts that corresponds to such transitions are of the same order of magnitude with the possible isotope shifts in the elements present in the astrophysical objects [13]. Any changes in the isotope abundances in these objects will be the systematic errors in the finding of α variation [26–28]. As suggested by Kozlov *et al* [13] it is possible to construct anchor lines, those are insensitive to the variation of abundances in the astrophysical objects, and probe lines, those are insensitive to the α variation. It is also possible to construct such lines by considering combinations of suitable transitions of the elements present inside the astrophysical objects [13]. To find out the sensitive lines to α variation and/or strong IS in any system, it is necessary to determine the α variation coefficient q and IS parameters, respectively, as defined explicitly below. Since both Na and Mg⁺ are proposed as suitable candidates for this purpose [24, 25], we would like to determine these properties accurately in the above systems.

There are three relativistic many-body methods have already been used to calculate the IS constants in the considered systems [28–30]. Safronova and Johnson have used at most two orders of Coulomb interactions through the third order many-body perturbation theory (MBPT(3) method) to calculate the ISs and the trends of different electron correlation effects are presented at this level of approximation [29]. Berengut *et al.* [30] have considered the IS operators in the atomic Hamiltonian with a varying parameter, then they calculate the energies self-consistently. Changes in the energies are estimated to the first order in that parameter to extract the corresponding ISs. However, it is not possible to find out the role of different electron correlation effects through this procedure. The individual field shift (FS) and specific mass shift (SMS) results reported by these two methods do not match well with each other although

*Email: bijaya@prl.res.in

the final ISs reported by both the works are close to the experimental measurements. This is due to the fact that there is a large cancellation between the initial state and final state results. However, it does not really explain the reason of discrepancies at the individual result. Korol and Kozlov [28] have followed approach considered by Dzuba *et al.* and present only the final results without giving details of the correlation contributions. Therefore, it is necessary to employ a relativistic many-body method that accounts correlation effects to all orders and it enables us to understand the underlying role of different correlation effects in these calculations. To fill-up the gap between the differences in the individual results reported by Safronova and Johnson and Berengut *et al.*, we follow an approach similar to Safronova and Johnson but consider atomic wavefunctions determined using the relativistic coupled-cluster (RCC) theory which is an all order perturbation method having size consistent property [31, 32]. The catagorily distinct features of this work are: (i) it will explain the differences between the results reported in [29] and [30], (ii) it will present individual contributions from various correlation (RCC) terms to both FS and SMS constant calculations and (iii) it will give q and ISs of many low-lying transitions in the considered systems those are not studied in the literature to date.

The remaining part of this paper is arranged as following: In the next section we will give the general theory of fine structure constant variation and ISs in the atomic systems. In the following section, we will explain the many-body techniques in the RCC framework that has been used to calculate the energies and IS properties. In Sec. IV, we will present the results and discuss them by comparing with the earlier results. In the last section, we will summarise our work and draw the conclusions.

II. THEORY

The IS (δE_v^{IS}) to an energy level of state $|\Psi_v\rangle$ in an atomic system is mainly classified into two parts: (a) the shifts (δE_v^{MS}) due to the consideration of finite nuclear mass that is known as mass shift (MS) and (b) the shifts (δE_v^{FS}) caused due to change in the nuclear charge radius from one isotope to another, known as FS. The MS can be further divided into normal mass-shift (NMS) and SMS. The NMS is given by

$$\delta E_v^{NMS} = -\frac{m_e}{m_e + M_A} E_v^{theory}$$

$$= -\frac{m_e}{M_A} E_v^{expt}, \quad (2.1)$$

where m_e and M_A are the electron and atomic masses, respectively. Here E_v^{theory} and E_v^{expt} are the respective energy levels of state v that can be theoretically calculated and experimentally observed, respectively. Accuracy in E_v^{theory} depends on the theoretical method employed in the calculations while accuracy of E_v^{expt} depends on the measurement techniques. For the considered systems, we use E_v^{expt} to estimate the corresponding NMSs.

The specific mass shift for the state $|\Psi_v\rangle$ is given by

$$\begin{aligned} \delta E_v^{SMS} &= -\frac{M_A}{2(m_e + M_A)^2} \langle \Psi_v | \sum_{i \geq j} \vec{p}_i \cdot \vec{p}_j | \Psi_v \rangle \\ &= -\frac{M_A}{(m_e + M_A)^2} \langle \Psi_v | Z | \Psi_v \rangle \\ &\simeq -\frac{1}{M_A} Z_v, \end{aligned} \quad (2.2)$$

where \vec{p}_i and \vec{p}_j and are the momenta of the electrons i and j , respectively. For the calculation point of view, we define Z as a two-body operator and express them in the second quantized notation as

$$Z = \frac{1}{2} \sum_{ab,cd} z_{abcd} a_a^\dagger a_b^\dagger a_d a_c, \quad (2.3)$$

with

$$z_{abcd} = \langle ab | \vec{p}_i \cdot \vec{p}_j | cd \rangle. \quad (2.4)$$

In the angular matrix form, we can have

$$\begin{aligned} z_{abcd} &= (-1)^{j_a - m_a + j_b - m_b} X(abcd) \sum_{q=-1,0,1} (-1)^q \\ &\begin{pmatrix} j_a & 1 & j_c \\ -m_a & q & m_c \end{pmatrix} \begin{pmatrix} j_b & 1 & j_d \\ -m_b & -q & m_d \end{pmatrix}, \end{aligned} \quad (2.5)$$

where the reduced matrix element is given by

$$\begin{aligned} X(abcd) &= \sqrt{(2j_a + 1)(2j_b + 1)(2j_c + 1)(2j_d + 1)} \\ &\begin{pmatrix} j_a & 1 & j_c \\ 1/2 & 0 & -1/2 \end{pmatrix} \begin{pmatrix} j_b & 1 & j_d \\ 1/2 & 0 & -1/2 \end{pmatrix} \\ &(-1)^{j_a + j_b + 1} R(ac)R(bd). \end{aligned} \quad (2.6)$$

Using the relation $|\vec{p}_i| = p_i = \frac{d}{dr_i} - \frac{\kappa_i}{r_i}$, we can have the expressions for the radial functions as

$$R(ij) = -i \int_0^\infty dr \left[P_i \left(\frac{dP_j}{dr_j} + \frac{\vartheta(\kappa_i, \kappa_j) P_j}{r_j} \right) + Q_i \left(\frac{dQ_j}{dr_j} + \frac{\vartheta(-\kappa_i, -\kappa_j) Q_j}{r_j} \right) \right], \quad (2.7)$$

where P_i and Q_i are the large and small components of

the Dirac orbital of electron i and the expression is valid

only for

$$\vartheta(\kappa_i, \kappa_j) = \begin{cases} -\kappa_j & \text{for } \kappa_i = \kappa_j - 1 \\ -\kappa_j & \text{for } \kappa_i = -\kappa_j \\ \kappa_j + 1 & \text{for } \kappa_i = \kappa_j + 1 \end{cases} \quad (2.8)$$

otherwise its value is zero.

$$R(ij) = -im_e c \int_0^\infty dr [(\kappa_i - \kappa_j - 1) P_i Q_j + (\kappa_i - \kappa_j + 1) Q_i P_j]. \quad (2.9)$$

Since the radial functions involved in both the expressions given by Eqs. (2.8) and (2.9) are different, they can be simultaneously used by a given many-body method to verify the numerical inaccuracies in the calculations.

For the field-shift calculation, we consider the nucleus is uniformly charged sphere of radius R with Z number of protons so that an electron in a distance r sees the nuclear potential

$$V_{nuc}(r, R) = \begin{cases} -(Z/2R)[3 - r^2/R^2] & \text{for } r < R \\ -Z/r & \text{for } r \geq R \end{cases} \quad (2.10)$$

This assumption will give reasonably accurate results for the considered light systems. In this case, the rms $\langle r^2 \rangle$ is given by

$$\langle r^2 \rangle = \frac{3}{5} R^2. \quad (2.11)$$

Now any change $\delta \langle r^2 \rangle^{A,A'}$ in $\langle r^2 \rangle$ for different isotopes A and A' cause FS and is given by

$$\delta E_{IS}^{FS} = -F \lambda^{A,A'} \quad (2.12)$$

where F is called as field shift constant and $\lambda^{A,A'}$ is an expansion of $\delta \langle r^2 \rangle^{A,A'}$ as

$$\lambda^{A,A'} = \sum_n \frac{C_n}{C_1} \delta \langle r^2 \rangle^{A,A'} \quad (2.13)$$

for C_n being the expansion coefficients which are given by Seltzer [33]. In the present studies, it is sufficient enough to neglect the higher terms and assume $\lambda^{A,A'} \simeq \delta \langle r^2 \rangle^{A,A'}$.

It can be shown from the above discussions that

$$\begin{aligned} F &= \left\langle \frac{\delta V_{nuc}(r, R)}{\delta \langle r^2 \rangle} \right\rangle \\ &= \begin{cases} -(5Z/4R^2)[1 - r^2/R^2] & \text{for } r \leq R \\ 0 & \text{for } r > R \end{cases} \end{aligned} \quad (2.14)$$

The above operator is a one-body scalar operator and its expectation value with respect to $|\Psi_v\rangle$ will give its FS constant, F_v .

The above expression can also be given in another form by using the relation $p_i = m_e c |\vec{\alpha}|$ with c is the velocity of light and $\vec{\alpha}$ being the Dirac matrix as

Finally, the IS of any transition between state i to state f of an isotope with mass number $M_{A'}$ to another isotope with mass number M_A is given by

$$\begin{aligned} \delta V_{if}^{A',A} &= \left(\frac{1}{M_{A'}} - \frac{1}{M_A} \right) [(E_i^{expt} - E_f^{expt}) + (Z_i - Z_f)] \\ &\quad + (F_i - F_f) \delta \langle r^2 \rangle^{A',A} \\ &= \frac{M_A - M_{A'}}{M_{A'} M_A} (k_{if}^{NMS} + k_{if}^{SMS}) + F_{if} \delta \langle r^2 \rangle^{A',A} \end{aligned} \quad (2.15)$$

In the literature, $k_{if}^{NMS} = E_i^{expt} - E_f^{expt}$, $k_{if}^{SMS} = Z_i - Z_f$ and $F_{if} = F_i - F_f$ are known as NMS constant, SMS constant and FS constant for the transition i to f , respectively.

In the context of α variation, the transition frequency observed from some distant astrophysical objects can be expanded in a series of α^2 at $\alpha = 0$ in the following way

$$\omega(x) = \omega^{(0)} + \alpha^2 \omega^{(0)} + \mathfrak{D}(\alpha^4). \quad (2.16)$$

For a fine-structure transition, the first coefficient is zero while it is finite for an optical transition. Therefore, the ratios of these transition frequencies can have different leading orders in α^2 . In an equivalent form, $\omega(x)$ can be expanded at $\alpha = \alpha_0$ for the laboratory value α_0 as

$$\omega(x) = \omega_{lab} + qx + \mathfrak{D}(x^2) \quad (2.17)$$

where ω_{lab} is the transition frequency in the present laboratory value and q is the α variation coefficient defined according to $x = (\alpha/\alpha_0)^2 - 1$. In principle, q can be determined from the first derivative $\frac{d\omega(x)}{dx}$ for small value of x and from a numerical calculation it can be assumed as

$$q \approx \frac{\omega(+\delta x) - \omega(-\delta x)}{2\delta x}. \quad (2.18)$$

For simplicity, if we assume $\delta x = 0.05$ then, we have

$$q \approx 10[\omega(+0.05) - \omega(-0.05)]. \quad (2.19)$$

III. METHOD OF CALCULATIONS

A. Wavefunction and energy calculations

For our purpose, we consider the Dirac-Coulomb Hamiltonian given by

$$H^{DC} = \sum_i [\alpha \vec{\alpha} \cdot \vec{p}_i + (\beta - 1)c^2 + V_{nuc}(r_i)] + \sum_{i>j} \frac{1}{r_{ij}}, \quad (3.1)$$

where we use atomic unit and consider the laboratory value of fine structure constant as $c = 1/\alpha_0 = 137.03599972$ in the present calculation. For α variation study, we consider different values of α in the above expression.

Since both Na and Mg⁺ are one valence configuration systems, we construct their atomic wavefunctions in the RCC framework as

$$|\Psi_v\rangle = e^T \{1 + S_v\} |\Phi_v\rangle, \quad (3.2)$$

where $|\Phi_v\rangle$ is the Dirac-Fock (DF) wavefunction that is constructed by appending a valence electron v to the DF wavefunction of the closed-shell configuration [$2p^6$] represented by $|\Phi_0\rangle$; i.e. $|\Phi_v\rangle = a_v^\dagger |\Phi_0\rangle$. Here T and S_v are the RCC operators that excite electrons from $|\Phi_0\rangle$ and $|\Phi_v\rangle$, respectively, due to the electron correlation effects that have been neglected in the DF method. The curly bracket with S_v operator represents it is in normal order form. Since both the considered systems are small in size, we approximate our RCC theory only for all possible single and double excitations by defining

$$\begin{aligned} T &= T_1 + T_2 \\ \text{and } S_v &= S_{1v} + S_{2v}, \end{aligned} \quad (3.3)$$

which is known as CCSD method.

The detailed equations to solve both T and S_v operator amplitudes are discussed in [34, 35]. The electron attachment energy or negative of the ionization potential (IP) is evaluated by

$$\Delta E_v = \langle \Phi_v | \overline{H}_N^{DC} \{1 + S_v\} | \Phi_v \rangle, \quad (3.4)$$

where $\overline{H}^{DC} = e^{-T} H^{DC} e^T$ and the normal order Hamiltonian is given by $H_N^{DC} = H^{DC} - \langle \Phi_0 | H^{DC} | \Phi_0 \rangle$. To improve the quality of the results, we construct the triple excitation RCC operator for S_v as

$$S_{3v}^{pert} = \frac{\widehat{H}_N^{DC} T_2 + \widehat{H}_N^{DC} S_{2v}}{\epsilon_v + \epsilon_a + \epsilon_b - \epsilon_p - \epsilon_q - \epsilon_r}, \quad (3.5)$$

and include its effects in Eq. (3.4) to evaluate energy which also enters into the CCSD amplitude determining equation for S_v . This approach is called as CCSD(T) method and it includes the most important part of the triple excitation effects. Here widehat symbol means the terms are connected and ϵ 's are the single particle energies of the orbitals (+ sign means for incoming orbitals and - sign means for out going orbitals) involved in the excitaions.

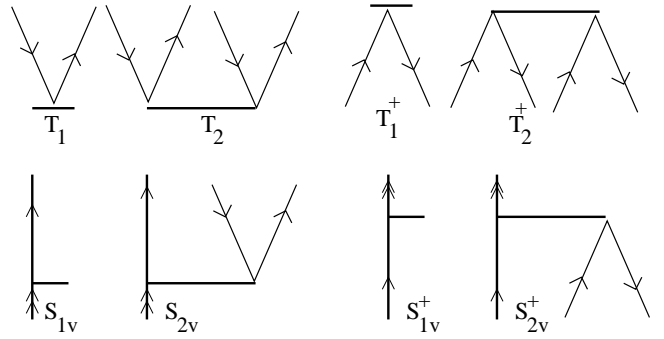


FIG. 1: Diagrammatic representation of the RCC operators along with their conjugates. Lines with single arrows going down represent the occupied (hole) orbitals, lines with single arrows going up represent the virtual (particle) orbitals and lines with double arrows represent the valence orbitals, respectively. Note that a particle line can be converted to a valence orbital in a special case, but not the other way around.

B. Properties evaluation

The expectation value of any physical operator O using the RCC method for a given state $|\Psi_v\rangle$ is evaluated by

$$\langle O \rangle_v = \frac{\langle \Phi_v | \{1 + S_v^\dagger\} e^{T^\dagger} O_N e^T \{1 + S_v\} | \Phi_v \rangle}{\langle \Phi_v | \{1 + S_v^\dagger\} e^{T^\dagger} e^T \{1 + S_v\} | \Phi_v \rangle}, \quad (3.6)$$

where $O_N = O - \langle \Phi_0 | O | \Phi_0 \rangle$ is the normal order form of O . We note that since both T and S_v are in normal order form and wavefunctions are calculated using H_N^{DC} , so it is necessary to consider O_N in the above expression; which will be necessary to note for the following discussions.

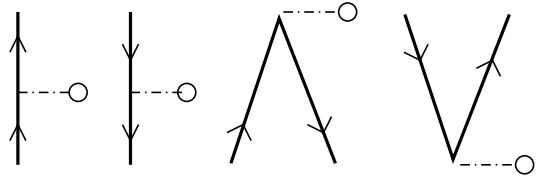


FIG. 2: Diagrammatic representations of any one-body operator "O" as per the definitions of lines used in Fig. 1.

Using the above method, there are a number of studies carried out on varieties of properties and the procedure to evaluate or approximate the non-truncative series like $e^{T^\dagger} O_N e^T$ and $e^{T^\dagger} e^T$ for the required accuracy of the results are given elsewhere (for example see [34, 35]). However, these calculations were only for the properties involving one-body operators. For the two-body SMS operator Z , the normal order form will have two parts $Z_N = Z_1 + Z_2$ which can be written as

$$\begin{aligned} Z_1 &= \sum_{i,j} z_{ij} \{a_i^\dagger a_j\} \\ \text{and } Z_2 &= \frac{1}{2} \sum_{ij,kl} z_{ijkl} \{a_i^\dagger a_j^\dagger a_l a_k\}, \end{aligned} \quad (3.7)$$

where the curly bracket means they are in normal order forms and the amplitudes of the effective one-body operator Z_1 is given by

$$\langle Z_1 \rangle_{ij} = z_{ij} = \sum_c [\langle ic|Z|jc \rangle - \langle ic|Z|cj \rangle]. \quad (3.8)$$

In the above expressions i, j, k and l indices used for any generic orbitals whereas c represents all the occupied orbitals. The DF result of this operator is determined by Z_1 by fixing its amplitude for $i = j = v$; for a given valence orbital v .

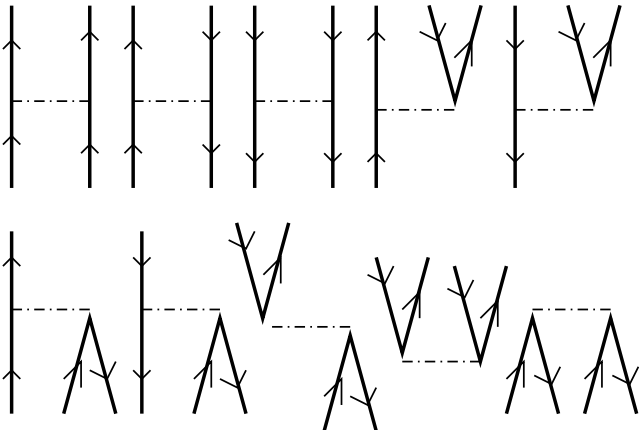


FIG. 3: Diagrammatic representation of Z_2 operator. Electron-electron Coulomb interaction (V_c) operator can be represented in the same way. To differentiate the notation between these two operators, we will use the dashed (-----) lines for V_c whenever it is necessary.

To evaluate contributions from $\bar{Z}_1 = e^{T^\dagger} Z_1 e^T$, we have considered the same procedure that is employed for the one-body operators [34, 35] as discussed above. We also follow a similar procedure to account contributions from $\bar{Z}_2 = e^{T^\dagger} Z_2 e^T$. First we evaluate the effective one-body terms from \bar{Z}_2 at the same level of approximations of \bar{Z}_1 and consider along with it. It can be noted that the effective two and three body terms from \bar{Z}_1 considered earlier [34, 35] are of at most fourth order in Coulomb interaction; otherwise they were neglected. In the present work, we also assume same approximation to evaluate the effective two and three body terms from \bar{Z}_2 ; however the number of Goldstone diagrams in this case increase drastically compared to the earlier case. We discuss below the crucial contributing effective one-body and two-body diagrams explicitly.

C. Goldstone diagrammatic representation

To understand the role of different correlation effects coming through various RCC terms, we express T and S_v operators diagrammatically in Fig. 1 with their corresponding conjugates. It has to be noted here that the core correlation effects are taken care through the T and

TABLE I: Different parameters (parm) used for the considered symmetries (l) for the wavefunction calculations in Na and Mg^+ . Here N^{GTO} and N^{CC} are the total number of GTOs used to generate the single particle orbitals and considered active orbitals for the RCC calculations, respectively.

parm \ l	0	1	2	3	4
$\eta_0 \times 10^2$	0.450	0.452	0.460	0.480	0.510
ζ	2.69	2.69	2.69	2.69	2.73
N^{GTO}	34	32	30	30	30
N^{CC}	13	13	12	11	9

its conjugate operators. The lower order pair-correlation effects and core-polarization effects involving the valence orbitals are accounted through S_{1v} and S_{2v} operators, respectively (for example see [34] and references therein).

There are only four general Goldstone diagrams representing any normal ordered one-body operator which are shown in Fig. 2. Therefore, the contributions from the FS operator F and one-body part of the SMS operator Z_1 will be described by these diagrams.

We also give the diagrammatic representation of the Z_2 operator in Fig. 3 and the Coulomb operator $V_c = \frac{1}{r_{ij}}$ can also be represented by similar diagrams.

Now using the above diagrammatic tools, we will be able to discuss the roles of various correlation effects.

TABLE II: Calculated IPs (in cm^{-1}) for different states in Na with different values of α .

Atomic state	IP with $\omega(0.0)$	IP with $\omega(+0.05)$	IP with $\omega(-0.05)$
$3s \ ^2S_{1/2}$	41345.396	41348.311	41342.485
$3p \ ^2P_{1/2}$	24461.150	24461.792	24460.506
$3p \ ^2P_{3/2}$	24442.953	24442.677	24443.230
$4s \ ^2S_{1/2}$	15676.945	15677.627	15676.262
$3d \ ^2D_{5/2}$	12269.785	12269.785	12269.784
$3d \ ^2D_{3/2}$	12269.738	12269.736	12269.740
$4p \ ^2P_{1/2}$	11148.860	11149.072	11148.648
$4p \ ^2P_{3/2}$	11142.482	11142.393	11142.571
$5s \ ^2S_{1/2}$	7708.343	7708.789	7707.896
$4d \ ^2D_{5/2}$	6781.742	6781.743	6781.742
$4d \ ^2D_{3/2}$	6781.702	6781.701	6781.703
$4f \ ^2F_{5/2}$	6847.330	6847.331	6847.329
$4f \ ^2F_{7/2}$	6847.323	6847.323	6847.322
$5p \ ^2P_{1/2}$	4930.127	4930.414	4929.841
$5p \ ^2P_{3/2}$	5117.936	5117.826	5118.047

IV. RESULTS AND DISCUSSIONS

A. Single particle orbitals

In the present calculations, we have used Gaussian type orbitals (GTOs) basis to construct the single particle orbitals which are given by

$$F_j^{GTO}(r_i) = r_i^{n_\kappa} e^{-\eta_j r_i^2} \quad (4.1)$$

where η_j is an arbitrary parameter which is again defined by two parameters as

$$\eta_j = \eta_0 \zeta^{j-1} \quad (4.2)$$

for j representing the number of GTOs ($F_j^{GTO}(r_i)$) considered for a given symmetry with the radial quantum number n_κ . The radial grid points to define these functions are generated using the relation

$$r_i = r_0 \left[e^{h(i-1)} - 1 \right] \quad (4.3)$$

where the starting grid point and the step size are considered as $r_0 = 2 \times 10^{-6}$ and $h = 0.03$, respectively, for a total number of grid points, represented by i , 750.

The above orbitals are also geneted by accounting the finite size of the nucleus assuming a two-parameter Fermi-nuclear-charge distribution that is given by

$$\rho(r_i) = \frac{\rho_0}{1 + e^{(r_i - c)/a}}, \quad (4.4)$$

where ρ_0 is the density for the point nuclei, c and a are the half-charge radius and skin thickness of the nucleus. These parameters are chosen as

$$a = 2.3/4(\ln 3) \quad (4.5)$$

and

$$c = \sqrt{\frac{5}{3} r_{rms}^2 - \frac{7}{3} a^2 \pi^2}, \quad (4.6)$$

where r_{rms} is the root mean square radius of the corresponding nuclei which is determined by

$$r_{rms} = 0.836 M_A^{1/3} + 0.570 \quad (4.7)$$

in fm for the atomic mass M_A . It should be noted that r_{rms} can also be obtained by combining the measured ISs with our calculated quantities for FS and MS, but we use the above approximation to calculate the final IS of many transitions where the experimental results are not available. Again both Na and Mg^+ have lighter nuclei, so the above approximation gives reasonably accurate r_{rms} values for the considered systems.

We have considered same η_0 , ζ and GTO parameters for different symmetries in both Na and Mg^+ in order to compare the trends of the correlation effects due to their nuclear sizes. Although a large number of GTOs are used

to produce the single particle orbitals, the higher energy orbitals do not contribute significantly in the RCC calculations but they increase the amount of computations. Therefore, we have considered only the required active orbitals along with all the occupied orbitals in the RCC calculations those play significant roles in the accurate determination of the considered properties. A brief summary of the considered parameters that are taken in the DF and RCC calculations are listed in Table I.

B. Results in Na

Using our RCC method, we calculate first IPs of several low-lying states for different values of α and they are given in Table II. In Table III, we report the excitation energies and q values for different transitions with respect to the ground state using the above IP results.

We have also compared our calculated excitation energies with their corresponding experimental results for the considered transitions in Table III. As seen, our results are of sub-one percent accurate for most of the transitions. Using the accuracy of the calculated excitation energies, we have also estimated the accuracy of the q values and given them in the parenthesis of the results. We have also compared our results with other available theoretical results in the same table for a few transitions reported by Berengut et al [24] using different many-body methods. As can be noticed, our results are more accurate than the results reported in [24].

We also find that some of the q values from the higher transitions are of same order of magnitudes with the low-lying transitions implying that the fine structure constant variation studies can also be carried out using these transitions in Na. It is also possible to use them to construct the anchor lines.

We have calculated F and Z using the same wavefunctions for different states those were used to evaluate the above IPs of the corresponding states. We have reported these results in Table IV. As discussed in Sec. II, it is possible to use the radial integrals given either by Eq. (2.7) or by Eq. (2.9) to evaluate the SMS constants. To verify the numerical accuracy in the SMS constant calculations, we have used both the expressions to evaluate them. We report results as Z I when we have used the expression given by Eq. (2.7) and as Z II when we have used the expression given by Eq. (2.9). Excellent agreement between the results obtained using both the expressions indicate high numerical accuracy in the calculations.

We have also given the available results for the same properties from the other works which were calculated using different relativistic many-body methods. Safronova and Johnson [29] have used two orders of Coulomb interaction in their MBPT(3) approach to evaluate these quantities whereas Berengut [30] have used a chain of diagrams through the Green's function technique with the Brueckner orbitals. The important difference between these two methods is that Safronova and Johnson have

evaluated the above properties from different correlation diagrams separately within MBPT(3) method whereas Berengut *et al* have considered both the FS and SMS interaction operators in the atomic Hamiltonian with a varying parameter and solved them self-consistently. By plotting various energies for different values of the parameters, they have extracted the IS constants. However, Berengut *et al* have scaled their wavefunctions to obtain the excitation energies matching with the experimental results and the same wavefunctions are used to estimate the above results. Obviously, this cannot explain the strength of the many-body method. In the calculations by Berengut *et al*, the contributions only from the large components (only the first term of the radial expression given by Eq. (2.7)) has been taken to calculate the SMS constants. Nevertheless, there is a large differences in the SMS results reported in [29] and [30]. The explanation given by Berengut *et al* for the possible reason of discrepancy between the two calculations that the MBPT(3) method may have poor convergence for the considered properties. In that case, it will be interesting to see how the all order calculations in the RCC approach match with their results.

It is seen from Table IV that our results for FS constants differ only little bit from the MBPT(3) results of Safronova and Johnson. However, there is a large difference in the SMS constant results between these works. Safronova and Johnson have given explicitly contributions from various correlation diagram within their MBPT(3) method and we discuss below explicitly the contributions from various RCC diagrams to both FS and SMS constants from where a comparison between the results at both the level approximations can be made. A careful analysis shows that the CCSD(T) method misses out some of the important triple excitation contributions to the SMS calculations through its two-body terms (Z_2) that contribute through the MBPT(3) method. To estimate these contributions, we have used the perturbed triple excitation RCC operator given by Eq. (3.5) in Eq. (3.6) and evaluated their contributions. These contributions are given in the parenthesis of our results for Z . As seen it seems though the large discrepancies between the MBPT(3) results and the CCSD(T) results are due to these contributions. It is possible that these extra triple excitation contributions may cancel with some of the quadrupole excitations, so we have not included these perturbative contributions in our final results instead consider them as possible source of errors for the determination of ISs as given below. Our SMS constant results match reasonably well with the results those are reported by Berengut *et al*, but they do not seem to agree each other after the inclusion of contributions from the triple excitations.

Substituting our calculated FS and SMS constants given in Table IV in Eq. 2.15 and using the experimental excitation energies given in Table III, we have calculated ISs for different transitions from the ground state between ^{22}Na – ^{23}Na and ^{23}Na – ^{24}Na . These re-

sults are given in Table V. We have calculated ISs using the SMS constants given by both Z I and Z II. Since the main source of errors in the IS calculations come from the SMS part, we have neglected the errors in FS and we present the recommended values (given as Reco in the above table) considering errors both from the numerical calculations and neglected correlation effects. There are three experimental measurements of ISs are available only for ^{22}Na – ^{23}Na in the $3s\ ^2S \rightarrow 3p\ ^2P_{1/2}$ and $3s\ ^2S \rightarrow 3p\ ^2P_{3/2}$ transitions [37–39]. The experimental values of IS in the $3s\ ^2S \rightarrow 3p\ ^2P_{1/2}$ transition are 758.5(7) MHz [37] and 756.9(1.9) MHz [38] and our result for this transition is well in agreement within its error bar. The experimental value of IS in the $3s\ ^2S \rightarrow 3p\ ^2P_{3/2}$ transition is 757.72(24) MHz [39] and our result is also in agreement with it. Recently, Korol and Kozlov have employed a hybrid many-body approach by combining the configuration interaction (CI) method with MBPT to calculate SMS constants and obtain IS as 775.8 MHz and 776.5 MHz for the $3s\ ^2S \rightarrow 3p\ ^2P_{1/2}$ and $3s\ ^2S \rightarrow 3p\ ^2P_{3/2}$ transitions after neglecting the FS contributions [28]. Nevertheless, our results match with all the studies and therefore our reported IS results in the other transitions can also be assumed to give correct predictions within their error bars. These results, indeed, will be useful for the experimentalists to carry out the IS measurements in these transitions. In fact, our SMS and FS constants can also be used to derive IS for other intercombination transitions.

C. Results in Mg^+

In Table V, we present the IPs of different low-lying states for Mg^+ with different values of α . The trend of the IPs are same with Na states when α changes from its laboratory value. From the IP results for $\alpha = \alpha_0$, we determine the calculated excitation energies for various transitions with respect to the ground state and have given them in Table VII along with their experimental results. We have also estimated q values from the IP results obtained from different α .

As seen from the above table, our excitation energies for the given transitions match well with the experimental results indicating that our calculations are very accurate. Using these accuracies, we have estimated the errors associated with the determined q values and they are given in the parenthesis in the same table. There are also calculations of q values available for the first two transitions which are given in the above table and unlike the results for Na, these results differ slightly from ours. By comparing Table III and Table VII, it is clear that the q values of the given transitions are larger in Mg^+ suggesting this candidate is more suitable than Na to carry out the fine structure variation study. Since both the laser cooling and ion trapping techniques are well advanced these days, very precise α variation measurement can be pursued in Mg^+ . Preliminary works by Batteiger

et al [40] on fine structure and IS measurements are the initial steps and recent motivation for the theorists towards such studies.

We have calculated the IS parameters in Mg^+ using the same wavefunctions those are used to calculate IPs of the corresponding states. They are presented in Table VIII. Again, we have determined SMS constants as Z I and Z II using different radial expressions as it has been discussed before. There is a large difference between both the results in Mg^+ where it was in excellent agreement for Na. This clearly indicates that the wavefunctions behave differently in both Na and Mg^+ although similar basis functions are used in both the systems except their different nuclear sizes.

We have also compared FS and SMS constants obtained from other works with ours in the above table. Unlike the case for Na, our results do not match well with the results obtained by Berengut et al [30]. The difference between their works and ours is already discussed in the previous subsection. It seems though our $3p$ results are close to the results obtained by Safronova and Johnson [29], but the SMS constant result for the ground state do not match at all from these two works. In fact after inclusion of the triple excitation effects perturbatively, as discussed in the previous subsection, the results do not seem to agree with any of the above works. In our calculations, these contributions from the perturbed triple excitation effects are considered as a possible source of errors in the calculations of SMS constants. The FS constant results between Safronova and Johnson and ours match reasonably except for the $3d$ states. Contributions from various correlation effects in the FS and SMS constant calculations through various RCC terms for this system are given explicitly below.

Using the above FS, SMS results and excitations energies given in Table VII, we have determined the ISs in various transitions with respect to the ground state between $^{24}\text{Mg}^+ - ^{25}\text{Mg}^+$ and $^{24}\text{Mg}^+ - ^{26}\text{Mg}^+$. These results are given in Table IX. There are experimental measurements of ISs available only in the $3s \ ^2S \rightarrow 3p \ ^2P_{1/2}$ and $3s \ ^2S \rightarrow 3p \ ^2P_{3/2}$ transitions between $^{24}\text{Mg}^+ - ^{26}\text{Mg}^+$ [40, 41] among which Batteiger et al [40] results are more recent and precise. The experimental values of IS in the $3s \ ^2S \rightarrow 3p \ ^2P_{3/2}$ transition are 3050(100) MHz [41] and 3087.560(87) MHz [40] and our result is in good agreement with them. The experimental values of IS in the $3s \ ^2S \rightarrow 3p \ ^2P_{1/2}$ transition are 3050(100) MHz [41] and 3087.560(87) MHz [40] and our result is also in agreement with them. Korol and Kozlov have obtained this result as 3086.3 MHz using the CI+MBPT approach and neglecting the FS contribution [28]. Agreement between all these results shows that our IS results reported for the other transitions will also be reasonable accurate and these results will guide any new experiments to measure IS in any of these transitions in the right direction. Using our FS and SMS constants from various states, it is also possible to determine IS in many more intercombination lines.

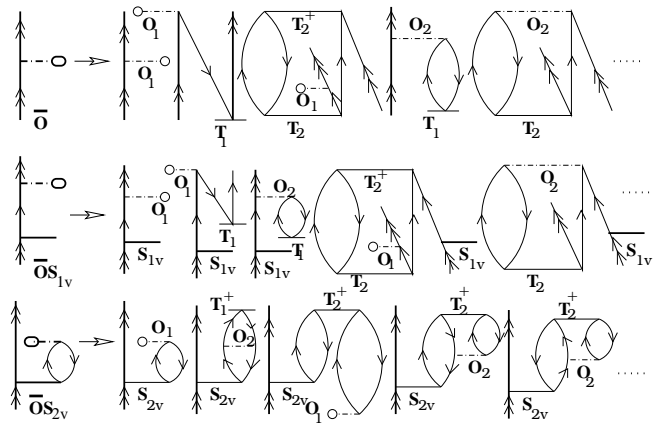


FIG. 4: Contributions from important RCC terms through the effective one-body operators.

D. Comparative studies of correlation effects

In Table X, we have reported contributions from DF and various RCC terms for the FS constant calculations of all the reported states both in Na and Mg^+ . This trend can be matched with the individual contributions reported by Safronova and Johnson [29] to find out how the all order correlation effects differ compared to MBPT(3). We have shown diagrammatically from the important contributing effective one-body RCC terms in Fig. 4 and expand the effective operators into a series of diagrams that contribute altogether through these terms (the diagrams coming from the two-body operator form of O do not contribute here). It is obvious from this figure that the difference between \bar{F} and F correspond to the core correlation effects which seem to be small for this property in both the systems. $\bar{F}S_{1v}$ and its conjugate terms account all order correlation effects from the pair-correlation type diagrams. Further, $\bar{F}S_{2v}$ and its conjugate terms consider all order correlation effects from the core-polarization diagrams. From the above table, we find that the pair correlation effects are stronger in the s states whereas the core-polarization effects play crucial role in obtaining the final results in all other states for FS constant calculations. Contributions from non-linear terms and normalization of the wavefunctions are given as "Others" and they seem to be small.

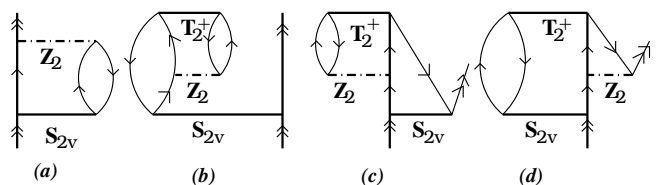


FIG. 5: Contributions from important effective two-body RCC terms to the specific mass shift calculations.

We present in Table XI the individual contributions to both Z I and Z II from various RCC terms for vari-

ous states in Na. Along with the contributions from the terms given for FS calculations, we also give the contributions from two-body term $Z_2 S_{2v}$ that contributes significantly in this calculation. The corresponding diagrammatic representation of this term is shown in Fig. 5(a). This seems to be a different types of pair correlation effects. As seen from the above table, the core correlation effects are sizably bigger in this property and the core-polarization effects coming through $\overline{Z_1} S_{2v}$ contribute larger than the pair correlation effects from $\overline{Z_1} S_{1v}$ with opposite sign. Contributions from $Z_2 S_{2v}$ are also larger than $\overline{Z_1} S_{1v}$ with opposite sign. As a result the final results have different signs than the DF results for most of states implying there are strong correlation effects in this property. In fact, there are also other non-linear two-body terms contribute significantly and their contributions are given by "Others" along with the contributions from normalization of the wavefunctions. Particularly the non-linear RCC terms of $T_2^\dagger Z_2 S_{2v}$ form contribute the most to "Others" and some of such diagrams are shown in Fig. 5(b-d).

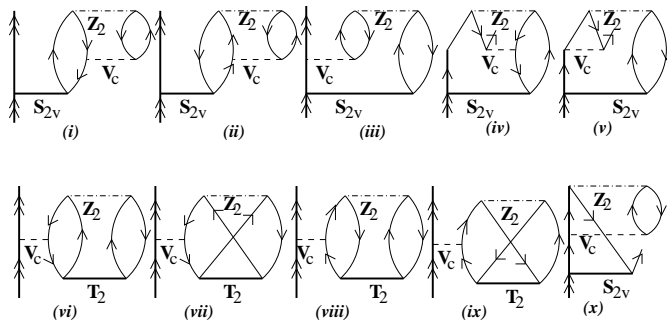


FIG. 6: Important triple excitation diagrams coming through S_{3v}^{pert} perturbative operator after contracting with Z_2 .

In Table XII, we present the contributions from different RCC terms, that are discussed above, to the SMS constant calculations for Mg^+ . There seem to be little larger differences at the DF results for Z I and Z II in this system. The trend of the results in this case is almost similar to Na, but the magnitudes are bigger for all the states.

In order to understand the role of triple excitation effects in the SMS constant calculations those do not appear at the CCSD(T) method, we have given contribu-

tions from the important perturbative terms in Table XIII whose diagrammatic representation are shown in Fig. 6. It is obvious from this table that the individual contributions from triple excitation effects are large, but the final contributions are small due to large cancellation among themselves. In fact, we believe that these results will also be further cancelled with the contributions from quadrupole excitations which was not possible to consider here due to their computational complexity. Again, triple excitation effects in Mg^+ seem to be larger than Na as per the magnitude of their final results. Contributions from triple excitations to FS constant calculations are very small compared to the CCSD(T) results due to the fact that it is a scalar one-body operator and these contributions have been neglected here.

V. SUMMARY

In summary, we have employed the relativistic coupled-cluster theory to estimate the fine structure constant variation coefficients for many transitions accurately in sodium and singly ionized magnesium. We have also calculated isotope shifts for the corresponding transitions in the considered systems. From these results, it is possible to construct suitable anchor and probe lines for the proposed fine structure constant variation studies in the above systems. We have also compared our results with other reported results obtained using different many-body approaches. By giving contributions from individual terms, we have shown explicitly the role of all order correlation effects in the isotope shift properties. We have also tried to understand the reasons for the differences in the results obtained from other calculations by finding contributions from important triple excitations. Our calculated results those are reported for the first time would be the bench mark results for the experimentalists to carry out their measurements in the right direction.

Acknowledgment

The author is grateful to V. Batteiger, M. Kozlov, M. Kowalska and B. P. Das for useful discussions and thanks V. Athalye for her help during this work.

[1] G. Breit, *Rev. Mod. Phys.* **30**, 507 (1958).
 [2] W. H. King, *Isotope Shifts in Atomic Spectra*, Plenum Press, New York (1984).
 [3] E. W. Otten, *Treatise on Heavy-Ion Science*, ed. by D. A. Bromley (Plenum, New York, 1989), vol. 8, p. 517.
 [4] T. Theodossiou, J. A. R. Griffith, J. L. Cookegig and D H Forest, *J. Phys. B: At. Mol. Opt. Phys.* **30**, L635 (1997).
 [5] E. W. Otten, *Hyperfine Int.* **2**,127 (1976).

[6] A. -M. Martensson and S. Salomonson, *J. Phys. B* **15**, 2115 (1982).
 [7] E. Lindroth, A.-M. Martensson-Pendrill and S. Salomonson, *Phys. Rev. A* **31**, 58 (1985).
 [8] A. -M. Martensson-Pendrill, D.S. Gough and P. Hanaford, *Phys. Rev. A* **49**, 3351 (1994).
 [9] F. Kurth *et al.*, *Z. Phys. D: At., Mol. Clusters* **34**, 227 (1995).

- [10] C. Froese Fischer, P. Jönsson and M. Godefroid, *Phys. Rev. A* **57**, 1753 (198).
- [11] B. Q. Chen and P. Vogel, *Phys. Rev. C* **48**, 1392 (1993).
- [12] K. Wendt, S. A. Ahmad, W. Klempt, R. Neugart, E. W. Otten and H. H. Stroke, *Z. Phys. D* **4**, 227 (1986).
- [13] M. G. Kozlov, V. A. Korol, J. C. Berengut, V. A. Dzuba and V. V. Flambaum, *Phys. Rev. A* **70**, 062108 (2004).
- [14] L. Broström, S. Mannervik, P. Royen and A. Wännström, *Phys. Scripta* **51**, 330 (1995).
- [15] *Particle Astrophysics, Atomic Physics and Gravitation*, ed. by J. T. Ván, G. Fontaine and E. Hinds, Moriond Workshops, Editions Frontieres, 91192 Gif-sur-Yvette Cedex-France (Singapore, 1994), p. 355.
- [16] K. A. Bronnikov and S. A. Kononogov, *Metrologia* **43**, R1 (2006).
- [17] J.K. Webb, M.T. Murphy, V.V. Flambaum, V.A. Dzuba, J.D. Barrow, C.W. Churchill, J.X. Prochaska and A.M. Wolfe, *Phys. Rev. Lett.* **87**, 091301 (2001).
- [18] Z. Chackoa, C. Grojeanc and M. Perelstein, *Phys. Lett B* **565**, 169 (2003).
- [19] R. Srianand, H. Chand, P. Petitjean and B. Aracil, *Phys. Rev. Lett.* **92**, 121302 (2004).
- [20] H. Chand, R. Srianand, P. Petitjean and B. Aracil, *Astron. Astrophys.* **417**, 853 (2004).
- [21] P. Tzanavaris, J. K. Webb, M. T. Murphy, V. V. Flambaum and S. J. Curran, *Phys. Rev. Lett.* **95**, 041301 (2005).
- [22] R. Quast, D. Reimers and S. A. Levshakov, *Astron. Astrophys.* **414**, L7 (2004).
- [23] A. Dzuba, V. V. Flambaum and J. K. Webb, *Phys. Rev. A* **59**, 230 (1999).
- [24] J. C. Berengut, V. A. Dzuba, V. V. Flambaum and M. V. Marchenko, *Phys. Rev. A* **70**, 064101 (2004).
- [25] V. A. Dzuba, V. V. Flambaum, M. G. Kozlov and M. Marchenko, *Phys. Rev. A* **66**, 022501 (2002).
- [26] S. A. Levshakov, *Mon. Not. R. Astron. Soc.* **269**, 339 (1994).
- [27] D. A. Varshalovich, A. Y. Potekhin and A. V. Ivanchik, *Phys. Scripta* **2001** (T95), 76 (2001).
- [28] V. A. Korol and M. G. Kozlov, *Phys. Rev. A* **76**, 022103 (2007).
- [29] M. S. Safronova and W. R. Johnson, *Phys. Rev. A* **64**, 052501 (2001).
- [30] J. C. Berengut, V. A. Dzuba and V. V. Flambaum, *Phys. Rev. A* **68**, 022502 (2003).
- [31] I. Lindgren and J. Morrison, *Atomic Many-body Theory*, ed. G. E. Lambropoulos and H. Walther (Berlin: Springer), vol. 3 (1985).
- [32] A. Szabo and N. S. Ostlund, *Modern Quantum Chemistry: Introduction to Advanced Electronic structure theory*, Dover Publications Inc., Mineola, New York, First edition (1996).
- [33] E. C. Seltzer, *Phys. Rev.* **188**, 1916 (1969).
- [34] B. K. Sahoo, *Phys. Rev. A* **80**, 012515 (2009).
- [35] D. Mukherjee, B. K. Sahoo, H. S. Nataraj and B. P. Das, *J. Phys. Chem. A* **113**, 12549 (2009).
- [36] http://physics.nist.gov/PhysRefData/ASD/levels_form.html
- [37] K. Pescht, H. Gerhardt and E. Matthias, *Z. Phys. A* **281**, 199 (1977).
- [38] G. Huber et al., *Phys. Rev. C* **18**, 2342 (1978).
- [39] Yu. P. Gangrsky et al., *Eur. Phys. J. A* **3**, 313 (1998).
- [40] V. Batteiger, S. Knünz, M. Herrmann, G. Saathoff, H. A. Schüssler, B. Bernhardt, T. Wilken, R. Holzwarth, T. W. Hänsch and Th. Udem, *Phys. Rev. A* **80**, 022503 (2009).
- [41] R. E. Drullinger, D. J. Wineland, and J. C. Bergquist, *Appl. Phys. (Berlin)* **22**, 365 (1980).

TABLE III: Excitation energies and q values in cm^{-1} for different states in Na.

Transition	Experiment	Others [24]		This work	
	EE [36]	EE	q	EE	q
$3s \ ^2S_{1/2} \rightarrow 3p \ ^2P_{1/2}$	16956.172	16858	45(4)	16884.246	45.4(2)
$3s \ ^2S_{1/2} \rightarrow 3p \ ^2P_{3/2}$	16973.368	16876	63(4)	16902.443	63.8(3)
$3s \ ^2S_{1/2} \rightarrow 4s \ ^2S_{1/2}$	25739.991			25668.451	44.6(2)
$3s \ ^2S_{1/2} \rightarrow 3d \ ^2D_{5/2}$	29172.839			29075.611	58.3(2)
$3s \ ^2S_{1/2} \rightarrow 3d \ ^2D_{3/2}$	29172.889			29075.658	58.3(2)
$3s \ ^2S_{1/2} \rightarrow 4p \ ^2P_{1/2}$	30266.990	30124	53(4)	30196.536	54.1(1)
$3s \ ^2S_{1/2} \rightarrow 4p \ ^2P_{3/2}$	30272.580	30130	59(4)	30202.914	60.1(2)
$3s \ ^2S_{1/2} \rightarrow 5s \ ^2S_{1/2}$	33200.675			33637.053	49.3(7)
$3s \ ^2S_{1/2} \rightarrow 4d \ ^2D_{5/2}$	34548.731			34563.654	58.3(1)
$3s \ ^2S_{1/2} \rightarrow 4d \ ^2D_{3/2}$	34548.766			34563.694	58.3(1)
$3s \ ^2S_{1/2} \rightarrow 4f \ ^2F_{5/2}$	34586.920			34498.066	58.2(2)
$3s \ ^2S_{1/2} \rightarrow 4f \ ^2F_{7/2}$	34586.920			34498.073	58.2(2)
$3s \ ^2S_{1/2} \rightarrow 5p \ ^2P_{1/2}$	35040.380			36415.269	52.5(2.1)
$3s \ ^2S_{1/2} \rightarrow 5p \ ^2P_{3/2}$	35042.850			36227.460	60.5(2.0)

TABLE IV: FS (in MHz/fm^2) and SMS (in $GHz \text{ } amu$) constants of many low-lying states in Na from different works.

Atomic state	Safronova [29]		Berengut [30]	F	This work	
	F	Z	Z		Z I	Z II
$3s \ ^2S_{1/2}$	-36.825	53.94	69	-37.044	71.4(-10.9)	72.8(-10.9)
$3p \ ^2P_{1/2}$	1.597	-43.36	-40	1.726	-40.5(-0.4)	-41.3(-0.4)
$3p \ ^2P_{3/2}$	1.603	-43.39	-39	1.765	-39.3(-3.3)	-39.2(-3.4)
$4s \ ^2S_{1/2}$				-8.555	20.7(-2.7)	21.0(-2.7)
$3d \ ^2D_{5/2}$	-0.062	-2.99		-0.051	-2.4(-0.4)	-2.4(-0.4)
$3d \ ^2D_{3/2}$	-0.062	-2.95		-0.049	-2.3(-0.2)	-2.3(-0.2)
$4p \ ^2P_{1/2}$				0.582	-14.5(-0.3)	-14.7(-0.3)
$4p \ ^2P_{3/2}$				0.596	-14.1(-1.2)	-14.1(-1.2)
$5s \ ^2S_{1/2}$				-5.546	14.4(-2.2)	14.6(-2.2)
$4d \ ^2D_{5/2}$				-0.028	-1.9(-0.2)	-1.9(-0.2)
$4d \ ^2D_{3/2}$				-0.027	-1.9(-0.1)	-1.9(-0.1)
$4f \ ^2F_{5/2}$				-0.004	0.2(0)	0.2(0)
$4f \ ^2F_{7/2}$				-0.004	0.2(0)	0.2(0)
$5p \ ^2P_{1/2}$				0.791	-19.8(-0.5)	-20.2(-0.6)
$5p \ ^2P_{3/2}$				0.755	-17.9(-1.5)	-17.9(-1.5)

TABLE V: Determination of ISs in MHz for Na. Results given as "Reco" are the recommended values after the numerical inaccuracies and neglected correlation effects in the calculations.

Transition	22-23			23-24		
	Z I	Z II	Reco	Z I	Z II	Reco
$3s^2S_{1/2} \rightarrow 3p^2P_{1/2}$	758.9	763.3	759(15)	699.4	703.4	699(15)
$3s^2S_{1/2} \rightarrow 3p^2P_{3/2}$	757.2	759.7	757(15)	697.7	700.1	698(15)
$3s^2S_{1/2} \rightarrow 4s^2S_{1/2}$	924.9	927.1	925(15)	852.6	854.6	853(15)
$3s^2S_{1/2} \rightarrow 3d^2D_{5/2}$	1079.0	1081.7	1079(20)	994.5	997.1	995(20)
$3s^2S_{1/2} \rightarrow 3d^2D_{3/2}$	1078.8	1081.5	1079(20)	994.3	996.9	994(20)
$3s^2S_{1/2} \rightarrow 4p^2P_{1/2}$	1138.9	1142.1	1140(20)	1049.8	1052.7	1050(20)
$3s^2S_{1/2} \rightarrow 4p^2P_{3/2}$	1138.4	1141.1	1140(20)	1049.3	1051.8	1049(20)
$3s^2S_{1/2} \rightarrow 5s^2S_{1/2}$	1194.7	1197.1	1195(15)	1101.3	1103.5	1101(15)
$3s^2S_{1/2} \rightarrow 4d^2D_{5/2}$	1255.7	1258.4	1256(20)	1157.4	1159.9	1157(20)
$3s^2S_{1/2} \rightarrow 4d^2D_{3/2}$	1255.7	1258.4	1256(20)	1157.4	1159.9	1157(20)
$3s^2S_{1/2} \rightarrow 4f^2F_{5/2}$	1249.4	1252.2	1249(15)	1151.7	1154.2	1152(15)
$3s^2S_{1/2} \rightarrow 4f^2F_{7/2}$	1249.4	1252.2	1249(15)	1151.7	1154.2	1152(15)
$3s^2S_{1/2} \rightarrow 5p^2P_{1/2}$	1350.7	1354.2	1351(20)	1245.0	1248.3	1245(20)
$3s^2S_{1/2} \rightarrow 5p^2P_{3/2}$	1340.8	1343.6	1341(20)	1236.0	1238.5	1236(20)

TABLE VI: Calculated IPs (in cm^{-1}) for different states in Mg^+ with different values of α .

Atomic state	IP with $\omega(0.0)$	IP with $\omega(+0.05)$	IP with $\omega(-0.05)$
$3s^2S_{1/2}$	121160.860	121170.521	121151.201
$3p^2P_{1/2}$	85538.955	85542.670	85535.245
$3p^2P_{3/2}$	85441.378	85440.205	85442.549
$4s^2S_{1/2}$	51418.868	51421.576	51416.161
$3d^2D_{5/2}$	49736.923	49736.855	49736.992
$3d^2D_{3/2}$	49736.186	49736.081	49736.290
$4p^2P_{1/2}$	40575.576	40576.861	40574.294
$4p^2P_{3/2}$	40550.112	40549.742	40550.481
$5s^2S_{1/2}$	28310.051	28311.277	28308.826
$4d^2D_{5/2}$	27845.866	27845.832	27845.902
$4d^2D_{3/2}$	27845.425	27845.368	27845.482
$4f^2F_{5/2}$	27433.775	27433.785	27433.766
$4f^2F_{7/2}$	27433.684	27433.687	27433.680
$5p^2P_{1/2}$	23523.731	23524.392	23523.071
$5p^2P_{3/2}$	23551.625	23551.443	23551.807

TABLE VII: Excitation energies and q values in cm^{-1} for different states of Mg^+ .

Transition	Experiment	Others [25]	This work	
	EE [36]	q	EE	q
$3s\ ^2S_{1/2} \rightarrow 3p\ ^2P_{1/2}$	35669.31	120	35621.905	119.0(2)
$3s\ ^2S_{1/2} \rightarrow 3p\ ^2P_{3/2}$	35760.88	211	35719.482	216.6(3)
$3s\ ^2S_{1/2} \rightarrow 4s\ ^2S_{1/2}$	69804.95		69741.992	139.1(1)
$3s\ ^2S_{1/2} \rightarrow 3d\ ^2D_{5/2}$	71490.19		71423.937	194.6(2)
$3s\ ^2S_{1/2} \rightarrow 3d\ ^2D_{3/2}$	71491.06		71424.674	195.3(2)
$3s\ ^2S_{1/2} \rightarrow 4p\ ^2P_{1/2}$	80619.50		80585.284	167.5(1)
$3s\ ^2S_{1/2} \rightarrow 4p\ ^2P_{3/2}$	80650.02		80610.748	200.6(1)
$3s\ ^2S_{1/2} \rightarrow 5s\ ^2S_{1/2}$	92790.51		92850.809	168.7(1)
$3s\ ^2S_{1/2} \rightarrow 4d\ ^2D_{5/2}$	93310.59		93314.994	193.90(1)
$3s\ ^2S_{1/2} \rightarrow 4d\ ^2D_{3/2}$	93311.11		93315.435	194.34(1)
$3s\ ^2S_{1/2} \rightarrow 4f\ ^2F_{5/2}$	93799.63		93727.085	193.0(2)
$3s\ ^2S_{1/2} \rightarrow 4f\ ^2F_{7/2}$	93799.75		93727.176	193.1(2)
$3s\ ^2S_{1/2} \rightarrow 5p\ ^2P_{1/2}$	97455.12		97637.129	180.0(4)
$3s\ ^2S_{1/2} \rightarrow 5p\ ^2P_{3/2}$	97468.92		97609.235	196.8(3)

TABLE VIII: FS (in MHz/fm^2) and SMS (in $GHz\ amu$) constants of many low-lying states in Mg^+ from different works.

Atomic state	Safronova		Berengut [30]	F	This work	
	F	Z	Z		$Z\ I$	$Z\ II$
$3s\ ^2S_{1/2}$	-116.01	38	83	-116.150	73.8(-18.7)	77.7(-18.9)
$3p\ ^2P_{1/2}$	9.800	-324	-296	10.126	-315.8(-2.8)	-320.7(-2.8)
$3p\ ^2P_{3/2}$	9.811	-323	-290	10.226	-311.7(-10.2)	-311.7(-10.3)
$4s\ ^2S_{1/2}$				-31.833	45.1(-5.3)	46.1(-5.3)
$3d\ ^2D_{5/2}$	-0.085	-106		-0.016	-100.5(-5.6)	-100.4(-5.6)
$3d\ ^2D_{3/2}$	-0.083	-105		-0.006	-99.6(-2.4)	-99.5(-2.4)
$4p\ ^2P_{1/2}$				3.470	-110.5(-1.8)	-112.2(-1.8)
$4p\ ^2P_{3/2}$				3.498	-109.2(-3.8)	-109.2(-3.9)
$5s\ ^2S_{1/2}$				-14.283	23.3(-2.4)	23.7(-2.4)
$4d\ ^2D_{5/2}$				0.035	-54.2(-3.1)	-54.2(-3.1)
$4d\ ^2D_{3/2}$				0.039	-53.8(-1.4)	-53.7(-1.4)
$4f\ ^2F_{5/2}$				-0.021	0.7(-0.1)	0.7(-0.1)
$4f\ ^2F_{7/2}$				-0.021	0.7(-0.1)	0.7(-0.1)
$5p\ ^2P_{1/2}$				1.777	-56.8(-1.1)	-57.7(-1.1)
$5p\ ^2P_{3/2}$				1.786	-55.9(-2.0)	-55.9(-2.1)

TABLE IX: Determination of ISs in MHz for Mg^+ . Results given as "Reco" are the recommended values after the numerical inaccuracies and neglected correlation effects in the calculations.

Transition	24-25			24-26		
	Z I	Z II	Reco	Z I	Z II	Reco
$3s^2S_{1/2} \rightarrow 3p^2P_{1/2}$	1603.9	1618.6	1604(25)	3077.0	3105.2	3077(40)
$3s^2S_{1/2} \rightarrow 3p^2P_{3/2}$	1599.7	1606.2	1600(40)	3069.0	3081.5	3069(60)
$3s^2S_{1/2} \rightarrow 4s^2S_{1/2}$	1946.6	1951.5	1947(25)	3735.3	3744.6	3735(40)
$3s^2S_{1/2} \rightarrow 3d^2D_{5/2}$	2229.7	2236.0	2230(25)	4278.2	4290.4	4278(40)
$3s^2S_{1/2} \rightarrow 3d^2D_{3/2}$	2228.2	2234.5	2228(25)	4275.4	4287.5	4275(40)
$3s^2S_{1/2} \rightarrow 4p^2P_{1/2}$	2497.3	2506.6	2497(30)	4791.8	4809.8	4792(50)
$3s^2S_{1/2} \rightarrow 4p^2P_{3/2}$	2495.8	2502.3	2496(30)	4789.0	4801.5	4789(50)
$3s^2S_{1/2} \rightarrow 5s^2S_{1/2}$	2614.2	2620.1	2614(30)	5016.5	5027.7	5017(50)
$3s^2S_{1/2} \rightarrow 4d^2D_{5/2}$	2753.6	2760.1	2754(30)	5283.8	5296.3	5284(50)
$3s^2S_{1/2} \rightarrow 4d^2D_{3/2}$	2752.9	2759.3	2753(30)	5282.5	5294.7	5283(50)
$3s^2S_{1/2} \rightarrow 4f^2F_{5/2}$	2673.2	2679.7	2673(30)	5129.5	5142.0	5130(50)
$3s^2S_{1/2} \rightarrow 4f^2F_{7/2}$	2673.2	2679.7	2673(30)	5129.5	5142.0	5130(50)
$3s^2S_{1/2} \rightarrow 5p^2P_{1/2}$	2876.3	2884.3	2876(30)	5519.3	5534.6	5519(50)
$3s^2S_{1/2} \rightarrow 5p^2P_{3/2}$	2874.0	2880.5	2874(30)	5514.9	5527.4	5515(50)

TABLE X: Comparative contributions from different RCC terms to the FS constants in Na and Mg^+ . \bar{F} is the effective one-body terms of $e^{T^\dagger} F e^T$. Contributions from the effective two-body and three-body terms of above non-truncative exponentials are given as "Others" along with the small contributions from normalization of the wavefunctions.

Atomic state	$\underline{DF(F)}$		\underline{F}		$\underline{FS_{1v} + c.c.}$		$\underline{FS_{2v} + c.c.}$		\underline{Others}	
	Na	Mg^+	Na	Mg^+	Na	Mg^+	Na	Mg^+	Na	Mg^+
$3s^2S_{1/2}$	-29.749	-104.686	-30.259	-105.838	-4.724	-9.264	-1.700	-0.693	-0.361	-0.355
$3p^2P_{1/2}$	-0.008	-0.059	0.032	0.042	0.003	3×10^{-4}	1.566	9.590	0.125	0.495
$3p^2P_{3/2}$	~ 0	~ 0	0.055	0.151	0.006	0.010	1.562	9.537	0.143	0.528
$4s^2S_{1/2}$	-7.239	-29.666	-7.347	-29.912	-0.818	-1.892	-0.326	0.088	-0.074	-0.117
$3d^2D_{5/2}$	~ 0	~ 0	7×10^{-5}	0.002	1×10^{-5}	2×10^{-4}	-0.047	-0.008	-0.004	-0.001
$3d^2D_{3/2}$	~ 0	~ 0	2×10^{-5}	3×10^{-4}	2×10^{-6}	2×10^{-5}	-0.047	-0.006	-0.002	2×10^{-4}
$4p^2P_{1/2}$	-0.003	-0.021	0.010	0.009	0.001	-0.001	0.534	3.316	0.037	0.145
$4p^2P_{3/2}$	~ 0	~ 0	0.017	0.045	0.002	0.002	0.534	3.297	0.043	0.154
$5s^2S_{1/2}$	-5.045	-13.539	-5.117	-13.641	-0.222	-0.670	-0.193	0.079	-0.014	-0.051
$4d^2D_{5/2}$	~ 0	~ 0	5×10^{-5}	0.001	6×10^{-6}	1×10^{-4}	-0.026	0.035	-0.002	-0.001
$4d^2D_{3/2}$	~ 0	~ 0	1×10^{-5}	1×10^{-4}	1×10^{-6}	1×10^{-5}	-0.026	0.036	-0.001	0.003
$4f^2F_{5/2}$	~ 0	~ 0	~ 0	3×10^{-6}	~ 0	~ 0	-0.003	-0.021	4×10^{-4}	-9×10^{-5}
$4f^2F_{7/2}$	~ 0	~ 0	~ 0	6×10^{-6}	~ 0	~ 0	-0.003	-0.021	4×10^{-4}	-9×10^{-5}
$5p^2P_{1/2}$	-0.004	-0.011	0.013	0.004	2×10^{-4}	-4×10^{-4}	0.748	1.706	0.030	0.066
$5p^2P_{3/2}$	~ 0	~ 0	0.022	0.022	0.001	0.001	0.697	1.693	0.035	0.070

TABLE XI: Contributions from different RCC terms to Z I and Z II in Na. \bar{Z} is again the effective one-body terms of $e^{T^\dagger} Z e^T$. Note that $Z = Z_1 + Z_2$ here. Important contributions from $Z_2 S_{2v}$ and its conjugate term are given explicitly. Other higher order contributions from effective two-body, three-body etc operators of the above non-terminating series with the normalization of the wavefunctions are given by "Others".

Atomic state	DF(Z_1)		\bar{Z}		$\bar{Z}_1 S_{1v} + c.c.$		$\bar{Z}_1 S_{2v} + c.c.$		$\bar{Z}_2 S_{2v} + c.c.$		Others	
	Z I	Z II	Z I	Z II	Z I	Z II	Z I	Z II	Z I	Z II	Z I	Z II
$3s \ ^2S_{1/2}$	-221.999	-221.633	-196.613	-196.195	-23.627	-23.571	163.268	164.040	74.726	74.760	53.683	53.785
$3p \ ^2P_{1/2}$	-115.614	-116.459	-117.300	-118.183	-18.601	-18.742	51.330	51.436	26.707	26.779	17.404	16.975
$3p \ ^2P_{3/2}$	-115.519	-115.740	-115.762	-115.988	-18.366	-18.404	50.786	51.054	26.696	26.756	17.349	17.350
$4s \ ^2S_{1/2}$	-49.485	-49.400	-43.613	-43.516	-3.130	-3.122	37.071	37.256	18.319	18.327	12.083	12.090
$3d \ ^2D_{5/2}$	-4.879	-4.880	-5.816	-5.817	-0.705	-0.705	1.888	1.895	-0.097	-0.096	2.354	2.357
$3d \ ^2D_{3/2}$	-4.845	-4.846	-5.771	-5.773	-0.700	-0.701	1.873	1.883	-0.101	-0.100	2.352	2.220
$4p \ ^2P_{1/2}$	-38.960	-39.244	-39.443	-39.739	-5.510	-5.552	16.560	16.594	8.827	8.851	5.108	5.108
$4p \ ^2P_{3/2}$	-39.021	-39.096	-39.041	-39.118	-5.460	-5.472	16.426	16.512	8.847	8.867	5.142	5.148
$5s \ ^2S_{1/2}$	-33.580	-33.523	-29.557	-29.492	-0.137	-0.136	24.679	24.795	12.583	12.588	6.827	6.836
$4d \ ^2D_{5/2}$	-3.510	-3.510	-4.183	-4.184	-0.462	-0.462	1.169	1.173	0.178	0.178	1.365	1.368
$4d \ ^2D_{3/2}$	-3.486	-3.487	-4.152	-4.153	-0.459	-0.459	1.158	1.165	0.172	0.173	1.356	1.357
$4f \ ^2F_{5/2}$	0.0	0.0	1×10^{-6}	1×10^{-6}	~ 0	~ 0	0.092	0.092	-0.101	-0.101	0.182	0.183
$4f \ ^2F_{7/2}$	0.0	0.0	3×10^{-6}	3×10^{-6}	~ 0	~ 0	0.091	0.092	-0.101	-0.101	0.183	0.183
$5p \ ^2P_{1/2}$	-55.689	-56.094	-56.330	-56.752	-4.579	-4.614	22.698	22.744	12.890	12.923	5.543	4.991
$5p \ ^2P_{3/2}$	-51.994	-52.094	-51.984	-52.086	-4.261	-4.271	21.006	21.116	12.046	12.072	5.272	5.276

TABLE XII: Contributions from different RCC terms to Z I and Z II in Mg^+ . \bar{Z} is as defined for Na. Important contributions from $Z_2 S_{2v}$ and its conjugate term are given explicitly. Other higher order contributions from effective two-body, three-body etc operators of the above non-terminating series with the normalization of the wavefunctions are given by "Others".

Atomic state	DF(Z_1)		\bar{Z}		$\bar{Z}_1 S_{1v} + c.c.$		$\bar{Z}_1 S_{2v} + c.c.$		$\bar{Z}_2 S_{2v} + c.c.$		Others	
	Z I	Z II	Z I	Z II	Z I	Z II	Z I	Z II	Z I	Z II	Z I	Z II
$3s \ ^2S_{1/2}$	-563.474	-562.198	-491.841	-490.453	-31.853	-31.751	367.573	369.704	155.300	155.426	74.612	74.740
$3p \ ^2P_{1/2}$	-599.456	-604.697	-601.684	-606.979	-61.947	-62.504	197.041	197.575	112.017	112.417	38.791	38.787
$3p \ ^2P_{3/2}$	-597.858	-599.283	-595.895	-597.356	-61.373	-61.534	194.989	196.228	111.680	112.015	38.929	38.970
$4s \ ^2S_{1/2}$	-137.727	-137.395	-119.996	-119.632	-4.302	-4.286	97.601	98.165	51.151	51.183	20.605	20.622
$3d \ ^2D_{5/2}$	-120.967	-120.988	-140.895	-140.932	-14.887	-14.892	23.333	23.420	16.100	16.120	15.895	15.916
$3d \ ^2D_{3/2}$	-120.263	-120.311	-139.972	-140.039	-14.822	-14.831	23.108	23.270	15.992	16.013	16.098	16.123
$4p \ ^2P_{1/2}$	-210.097	-211.898	-210.681	-212.527	-18.068	-18.231	66.176	66.359	40.079	40.218	11.961	11.955
$4p \ ^2P_{3/2}$	-209.467	-209.969	-208.762	-209.278	-17.899	-17.947	65.497	65.910	39.939	40.057	12.028	12.034
$5s \ ^2S_{1/2}$	-60.074	-59.927	-52.339	-52.178	-1.102	-1.097	43.551	43.802	24.170	24.184	9.032	9.037
$4d \ ^2D_{5/2}$	-66.429	-66.441	-77.396	-77.418	-7.602	-7.604	11.985	12.028	11.232	11.244	7.566	7.575
$4d \ ^2D_{3/2}$	-66.071	-66.099	-76.921	-76.960	-7.575	-7.579	11.867	11.951	11.169	11.181	7.665	7.674
$4f \ ^2F_{5/2}$	0.0	0.0	9×10^{-5}	9×10^{-5}	4×10^{-6}	4×10^{-6}	0.749	0.753	-1.465	-1.465	1.387	1.389
$4f \ ^2F_{7/2}$	0.0	0.0	2×10^{-4}	2×10^{-4}	8×10^{-6}	8×10^{-6}	0.753	0.757	-1.473	-1.473	1.384	1.387
$5p \ ^2P_{1/2}$	-108.722	-109.654	-109.041	-109.996	-8.459	-8.535	33.751	33.846	20.979	21.051	5.987	5.982
$5p \ ^2P_{3/2}$	-108.340	-108.600	-107.987	-108.254	-8.149	-8.171	33.359	33.569	20.893	20.953	5.933	5.934

TABLE XIII: Contributions from some of the important triple excitations coming through the contraction of S_{3v}^{pert} and Z_2 operators.

Atomic state	$3s^2S_{1/2}$		$3p^2P_{1/2}$		$3p^2P_{3/2}$		$3d^2D_{3/2}$		$3d^2D_{5/2}$	
	Na	Mg ⁺	Na	Mg ⁺	Na	Mg ⁺	Na	Mg ⁺	Na	Mg ⁺
Diag. (i)	-3.596	-9.191	-1.795	-7.057	-1.795	-7.052	-0.050	-0.438	-0.050	-0.436
Diag. (ii)	-10.960	-15.098	-4.553	-10.008	-4.553	-9.998	-0.251	-1.606	-0.251	-1.604
Diag. (iii)	16.895	31.263	3.934	10.260	1.908	4.283	0.306	2.737	0.205	1.924
Diag. (iv)	-3.896	-9.512	-1.565	-5.952	-1.588	-6.034	-1×10^{-4}	-0.008	-1×10^{-4}	-0.008
Diag. (v)	-4.916	-10.144	-0.157	-1.136	0.609	1.792	-0.003	-0.081	-0.030	-0.626
Diag. (vi)	650.914	878.079	458.160	718.768	457.730	717.810	253.550	480.306	253.554	480.327
Diag. (vii)	-137.896	-180.893	-96.981	-147.981	-96.890	-147.783	-53.611	-98.642	-53.611	-98.646
Diag. (viii)	-646.518	-868.182	-456.165	-711.433	-455.733	-710.482	-253.546	-480.185	-253.549	-480.206
Diag. (ix)	136.936	178.805	96.575	146.549	96.483	146.351	53.609	98.603	53.610	98.607
Diag. (x)	-10.803	-15.444	0.150	0.004	0.765	1.455	-0.068	-0.731	-0.186	-2.590